ADVANCED FUNCTIONAL MATERIALS
www.afm-journal.de

Microwave-Assisted Surface Synthesis of a Boron–Carbon–Nitrogen Foam and its Desorption Enthalpy

*Rajib Paul, Andrey A. Voevodin, Dimitry Zemlyanov, Ajit K. Roy, and Timothy S. Fisher**

The modification of microporous carbon foam with boron and nitrogen through a facile microwave chemical treatment are reported. The resulting surfaces of the foam exhibit distinct B–N and carbon domains based on chemical and microscopic analysis, in keeping with theoretical predictions. The resultant materials are shown to exhibit exceptionally high methanol desorption enthalpy and thermal stability in comparison to untreated carbon foam and consequently are suggested as candidate materials for sorption cooling and thermal storage applications using methanol as the adsorbate.

1. Introduction

A microwave-assisted thermo-chemical surface treatment of highly porous carbon foam has been developed to synthesize boron-carbon-nitrogen (B-C-N) foam for thermal energy storage and release by adsorption/desorption with lightweight hydrocarbons. Carbon foams provide the combined advantage of large surface area and high thermal conductivity critical for thermal energy storage, but they are prone to oxidation and have low adsorption enthalpy for lightweight hydrocarbons. The non-plasma microwave heating of the carbon foams exposed to boric acid and urea solutions described herein converts carbon foam to B-C-N foam. Microwave treatment helps to activate surface chemical reactions, and X-ray photoelectron spectroscopy reveals the formation of boron nitride and carbon nitride interatomic bonds with evidence of boron carbide bonds. This complex surface chemical structure is proposed to increase methanol desorption enthalpy, which in turn is expected to offer improved performance in adsorptive thermal applications.

B-C-N is a hexagonal solid material that can provide the benefits of intrinsically layered solids such as graphite and graphene,[1–3] with an additional advantage of higher thermal stability and wider band gap typical for hexagonal BN and BN nanosheets.[4] Many prior studies have considered the hybrid phases of B-C-N.[5–12] The synthesis procedures to produce B-C-N materials include r.f. plasma-enhanced pulsed laser deposition,[6] magnetron sputtering,[7,8] ion beam sputtered deposition,[9] arc discharge,[10] and chemical vapor deposition.[11,12] These studies have shown that B-C-N materials are not single crystalline but rather nanocrystalline.[13] Han et al. adopted chemical substitution reactions to replace C atoms in carbon nanotubes by B and N atoms to produce $(BN)_xC_y$ nanotubes.[14] This technique demonstrates a cost effective way to produce B-C-N material for which stability and electronic properties were theoretically predicted by density functional theory to depend primarily on chemical composition instead of the geometric structure.[15] However, B-C-N sheets have been shown to prefer conformations consisting of distributed BN and graphene domains, as opposed to spatially uniform stoichiometry, and the overall properties can depend on the details of the domain structure and distribution.[16]

Adsorption of light weight hydrocarbon has crucial importance for thermal storage and cooling applications, which utilize waste heat and can reduce adverse impact on global warming caused by the CFC refrigerants.[17] In adsorption cooling the choice of the adsorbate-adsorbent material pair determines the amount of thermal enthalpy per unit mass or volume.[18,19] Researchers have used activated carbon, activated alumina, zeolite, silica gel,[20] and calcium chloride[21] as adsorbents with water, ammonia, carbon dioxide, methanol, ethanol, andethylene as adsorbates for efficient sorption thermal processes. While these adsorbent/adsorbate pairs provide high values of enthalpy, their performance is often hindered by limitations of heat and mass transfer rates. From this perspective open porous structures with high thermal conductivity such as carbon foams and B-C-N foams may offer an advantage. Recently, Raidongia et al. measured adsorption of CO_2 (100%) by a 2–3 layer graphene-like B-C-N sheet synthesized by chemical substitution reactions.[22] Based on the general theory of adsorption in high-porosity adsorbents[23], B-C-N foam would appear to be a promising adsorbent with superior practical behavior in conjunction with chemically hazardless methanol adsorbate.[20]

Here we report microwave-assisted chemical substitution reactions to replace carbon atoms with boron and nitrogen to form an oxygen-resistant layer of B-C-N on the surface of pitch-derived graphitic carbon foam, which offers high porosity and stability.[24,25] A 400 W microwave treatment for 5–30 minutes was used to accelerate foam surface modification by 12–15 times in comparison to thermal treatments, due to activation of reagents through phase change and high thermal gradients during microwave irradiation.[26] The microwave treatment was followed by high-temperature annealing in an inert atmosphere

Dr. R. Paul, Dr. A. A. Voevodin, Dr. D. Zemlyanov, Prof. T. S. Fisher
Birck Nanotechnolgy Center
Purdue University
West Lafayette, IN 47907, USA
E-mail: tsfisher@purdue.edu
Dr. A. A. Voevodin, Dr. A. K. Roy, Prof. T. S. Fisher
Materials and Manufacturing Directorate
Air Force Research Laboratory
WPAFB, OH 45433, USA

DOI: 10.1002/adfm.201200325

to complete carbon foam surface conversion to B-C-N and to reduce excess oxygen content. The resultant material chemistry, morphology and structure are characterized in detail and correlated with methanol adsorption and thermal stability.

2. Results and Discussion

The surface morphology of as-received graphitic carbon foam is smooth and featureless as shown in **Figure 1**a. Figure 1b shows the surface of the foam after microwave-assisted chemical treatment for 5 min before annealing. Figure 1c,d contain SEM images of the B-C-N foams after 5 min microwave treatment and annealing at 500 °C and 1100 °C respectively. The images for the B-C-N foams after 30 min microwave treatment and annealing at 500 °C and 1100 °C are shown in Figure 1e and f respectively. The surfaces of B-C-N foams annealed at higher temperature (1100 °C) clearly exhibit increased roughness. A pronounced change in material morphology between B-C-N foams with 5 min and 30 min microwave treatment is also evident from SEM images (Figure 1d,f). From comparison of the surface morphology it is clear that both increased microwave treatment time and increased annealing temperature lead to topographic roughening, which would ostensibly enhance surface adsorption.

XPS analysis was used to investigate the conversion of carbon foam to B-C-N caused by microwave-assisted thermo-chemical treatment. The chemical reactions during the process can be expressed as follows[22]

$$2B(OH)_3 = B_2O_3 + 3H_2O$$

$$CO(NH_2)_2 = NH_3 + HNCO$$

$$B_2O_3 + 2NH_3 + 2xC = 2BC_xN + 3H_2O, [x = 1, 2.4] \quad (1)$$

Boron oxide is an intermediate constituent in the conversion process and was specifically targeted for the process optimization. The values of x (1, 2, 4), in Equation 1, can be used to determine the B-C-N structure. For example, $x = 2$ for BC_2N configuration. **Figure 2**a compares XPS survey spectra obtained from carbon foam before chemical treatment and foam subjected to the chemical treatment for 30 min and annealed at 1100 °C. Boron, nitrogen and oxygen appeared additionally in the treated foams. The atomic percentage of B, N and O additions varied with both microwave treatment time and annealing temperature as shown in Figure 2b–d. It is clear that an optimum temperature for maximizing boron and nitrogen content occurs within the 900–1100 °C range for both microwave treatment times. This temperature was found sufficient to induce the formation of B-N and C-N bonding (discussed below).

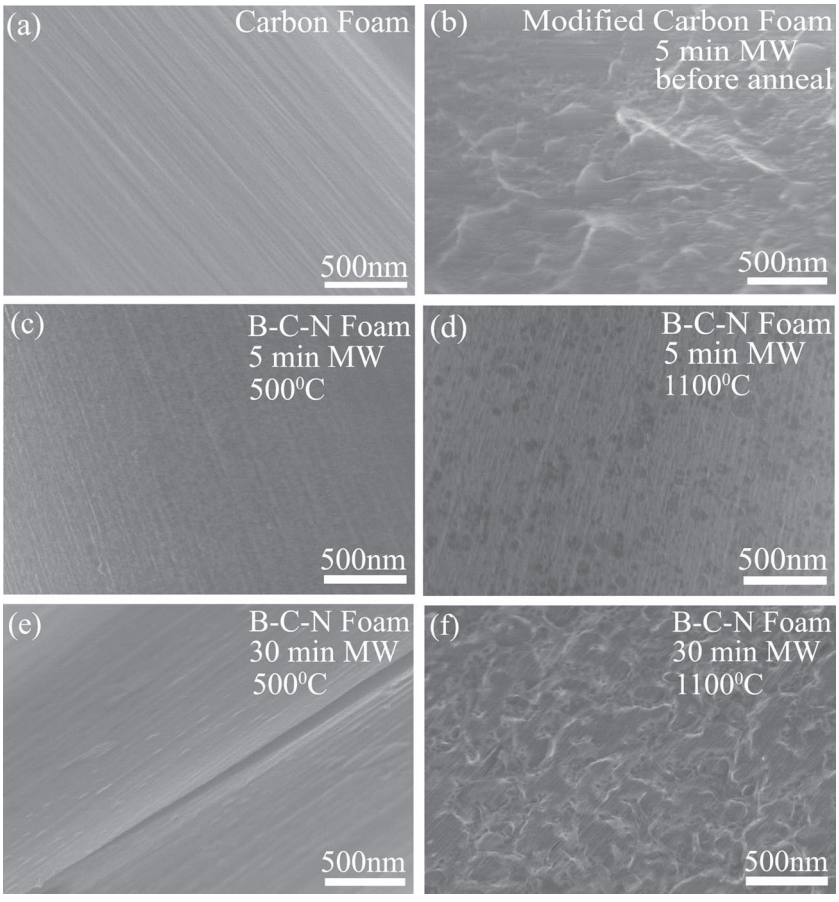

Figure 1. FESEM images of a) carbon foam, b) 5 min microwave treated carbon foam before annealing, c) 5 min microwave treated B-C-N foam annealed at 500 °C, d) 5 min microwave treated B-C-N foam annealed at 1100 °C, e) 30 min microwave treated B-C-N foam annealed at 500 °C, and f) 30 min microwave treated B-C-N foam annealed at 1100 °C.

Several chemically treated (at room temperature and atmospheric pressure) foam samples without microwave assistance were subjected to similar temperature and annealing profiles, but the B and N content of those foam samples were found to be negligible. Portechault et al.[27] used higher temperature (1400 °C or above) annealing in order to incorporate increased B and N molecules into mesoporous B-C-N. For the same purpose we annealed our chemically treated samples (treated at room temperature and atmospheric pressure) to 1500 and 1800 °C without preliminary microwave treatment. However, such process resulted in a very little B and N incorporation, indicating the critical role of the microwave treatment for the chemical reaction activation.

Figure 3 provides comparison of the C *1s* high-resolution XPS spectra obtained from the foams subjected to different annealing temperatures after 30 min microwave treatment. From this comparison, it is evident that the annealing temperatures of 500 and 700 °C were not sufficient to dissociate and remove HNCO, NCO_2 and other intermediate products of the chemical treatment reactions listed in Equation 1, and the carbon foam ligaments (inset of Figure 3) remained crystalline even after chemical treatment and annealing. At temperatures of 900 °C and

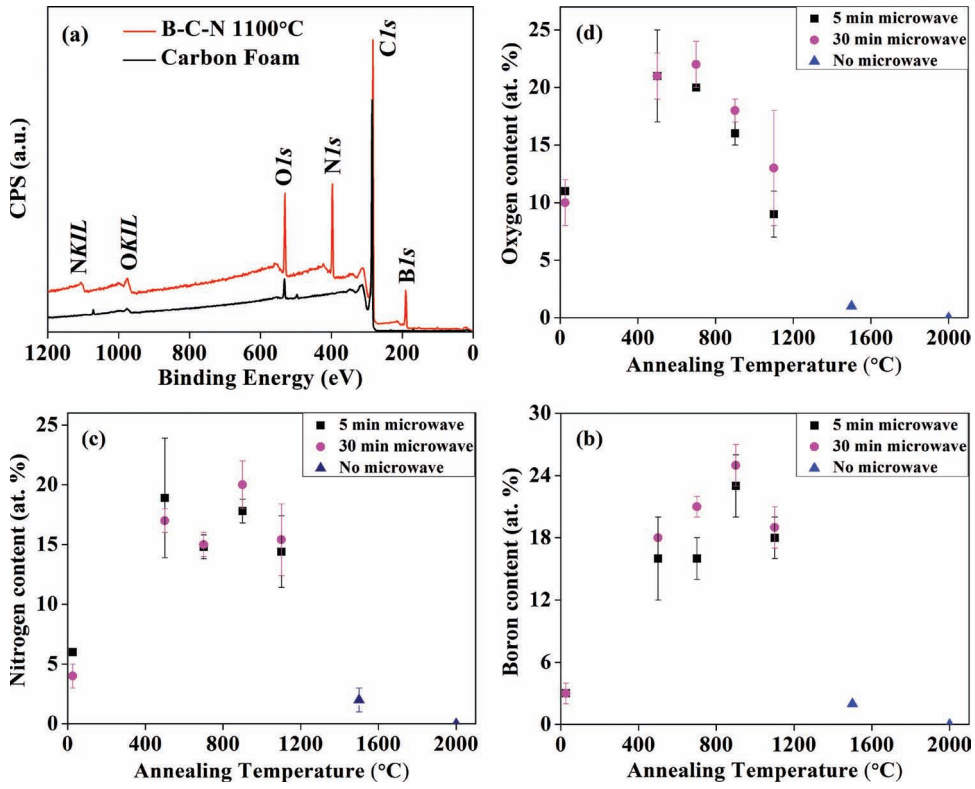

Figure 2. a) XPS spectra of carbon foam before treatment and B-C-N foam annealed at 1100 °C after 30 min microwave treatment. b–d) variations of B, N and O content (at%) within B-C-N foam with annealing temperature respectively for 5 min and 30 min microwave treatment.

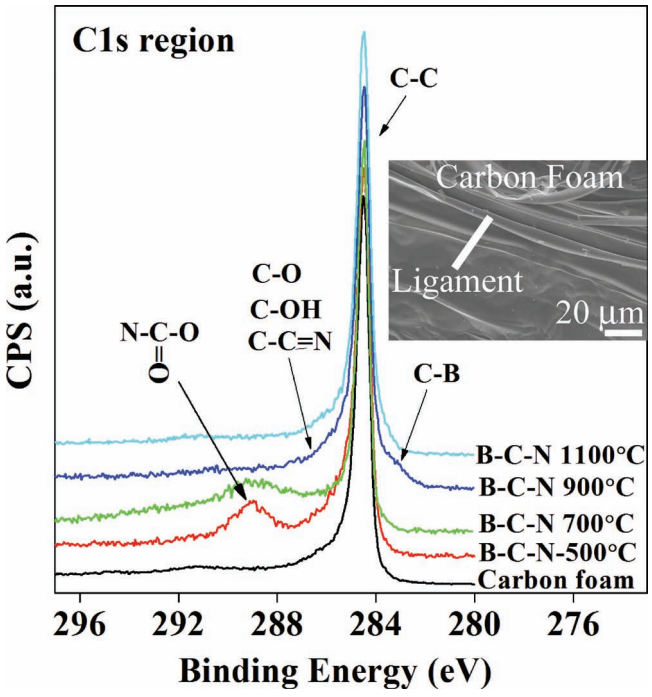

Figure 3. C *1s* spectra of carbon foam and B-C-N foams annealed at different temperatures after 30 min microwave treatment. Inset: ligament of carbon foam.

above, the C *1s* peak was composed mostly of C-C and C-N components with additional broadening due to disorder and a possible C-O contribution. Interestingly, for 900 °C annealing, a shoulder at the lower binding energy was apparent. This indicated possible boron carbide formation, as carbides typically have C *1s* peak at lower bonding energy relative to graphitic carbon.[28] This lower binding shoulder was weak and decreased at higher annealing temperatures.

Evaluation of the B *1s* and N *1s* high-resolution spectra had helped to reveal the critical role of annealing temperature in developing boron nitride bonds in the foams. **Figure 4**a shows the evolution of the B *1s* XPS spectra with increased annealing temperature for samples microwave treated for 30 minutes. The spectra were fitted with three components centered at 193.0 eV, 191.6 eV, and 189.9 eV which correspond to boron oxide, boron nitride, and boron carbide, respectively.[29–31] The figure shows a gradual replacement of boron oxide with boron nitride and boron carbide as the annealed temperature increases from 500 to 1100 °C. The observed consumption of B_2O_3 in favor of B-C-N conforms to the proposed chemical reaction mechanisms in Equation 1. Interestingly, this change was also accompanied by the N *1s* spectra evolution from that of predominantly C-N bonding to B-N bonding as temperature increased. This evolution is shown in Figure 4b, where fitting components were located at 400.7 eV, 398.5 eV, and 397.4 eV corresponding to nitrogen-carbon bonding in a pyridine-like configuration, in a graphite-like (or carbon substitution)

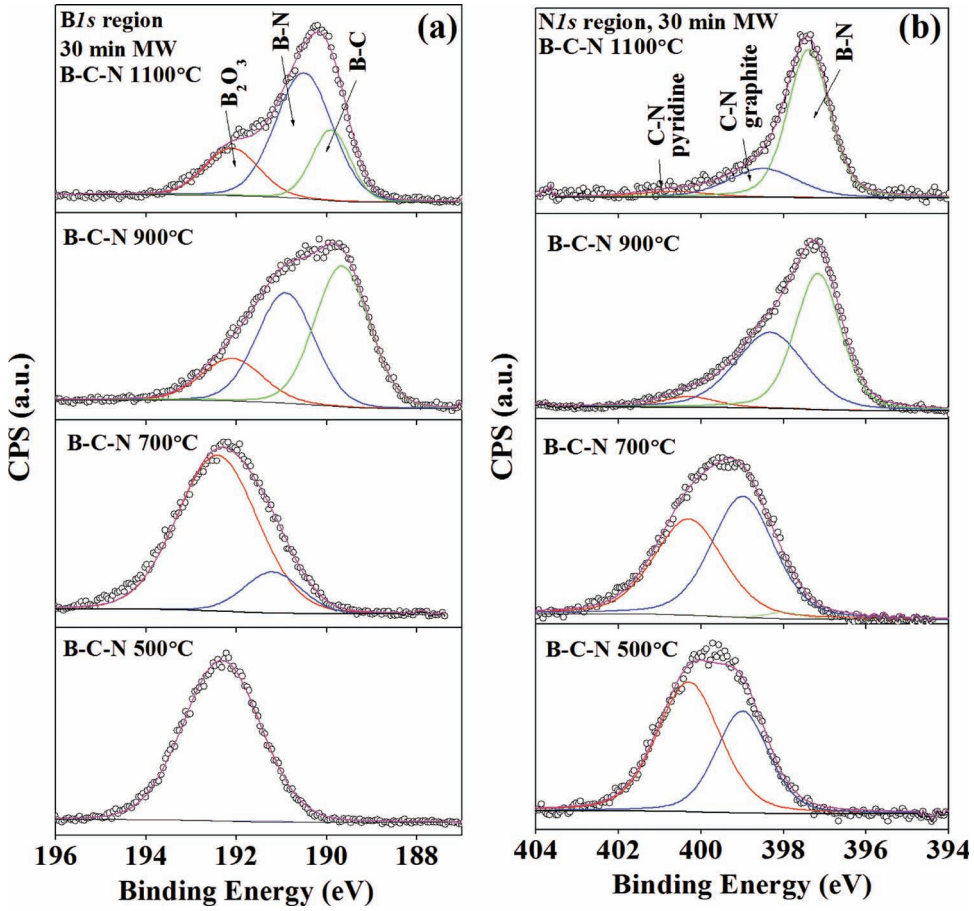

Figure 4. a) Deconvoluted B *1s* spectra for B-C-N foams treated for 30 min with microwave heating and annealed at different temperatures. b) Deconvoluted N *1s* spectra for B-C-N foams treated for 30 min with microwave heating and annealed at different temperatures.

configuration, and a nitrogen bond with boron, respectively.[29,31,32] We conclude based on these results that the prevalence of B-N bonded domains in the B-C-N foams increases with annealing temperature.

Table 1 presents the atomic percentage of boron in B-O, B-C, and B-N as a function of annealing temperature. From this table, the percentage of boron from boron nitride domains, as opposed to boron oxide, peaks at 10-11 at% for annealing temperatures of 900–1100 °C. Significantly, the 30 minute microwave treatment correlates to formation of boron carbide bonds at higher annealing temperatures, while for the 5 min treatment boron carbide bonds were absent for all annealing temperatures. Similarly, the percentage of nitrogen in B-N (Table 1) closely matches to that of boron with a nearly one-to-one ratio. This finding supports the conclusion that formation of B-N domains has occurred, as opposite to a random substitution of carbon with boron and nitrogen atoms upon the conversion of carbon foams to B-C-N foams.

The table also indicates that the fraction of nitrogen in the C-N pyridine-like position decreases with B-N domain growth, and 4–9 at% nitrogen remains bonded with carbon in a graphite-like configuration. Thus, the resulting B-C-N foams

Table 1. Boron and nitrogen content distribution of boron engaged in B-O, B-N, and B-C bonds, and nitrogen engaged in C-N pyridine-like, N-C graphite-like, and B-N bonding for the foams microwave processed for 5 min and 30 min and annealed to different temperatures.

Treatment time [min]	Annealing Temp [°C]	B in B-O [at%]	B in B-N [at%]	B in B-C [at%]	N in C-N pyridine [at%]	N in C-N graphite [at%]	N in B-N [at%]	Foam stoichiometric formula
5	500	15	1	0	3	13	2	$B_{0.71}C_{2.31}N_1$
5	900	12	10	0	2	5	10	$B_{1.13}C_{2.4}N_1$
5	1100	8	10	0	1	5	8	$B_{1.18}C_{4.12}N_1$
30	500	17	0	0	10	7	0	$B_{0.88}C_{2.66}N_1$
30	900	4	10	12	1	9	10	$B_{1.2}C_{1.85}N_1$
30	1100	4	11	4	1	4	11	$B_{1.22}C_{3.6}N_1$

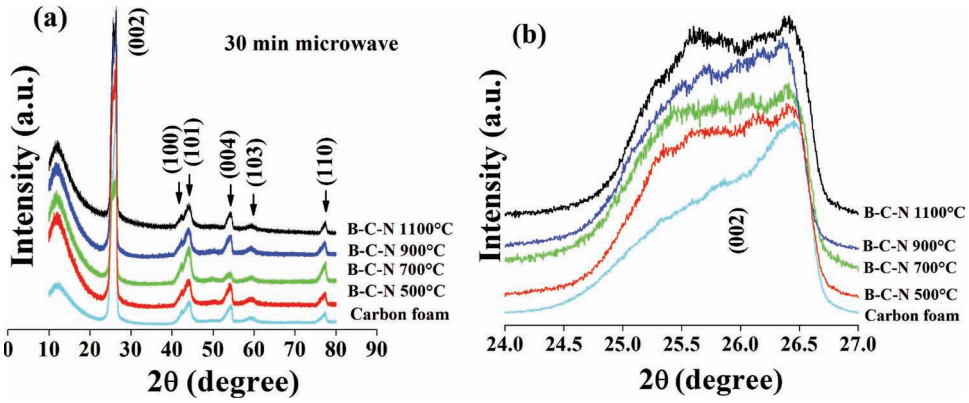

Figure 5. a) XRD spectra and b) (002) diffraction peak of B-C-N foams annealed at different temperatures treated with 30 min microwave heating.

consist of predominantly B-N and carbon domains, with the latter containing some substitution with nitrogen. The last column in Table 1 compares foam stoichiometric formulas, which vary between BC_2N and BC_4N for annealing temperature of 900 °C and above. It was observed that the percentage ratio of B-N and N-B are as obtained respectively from the B *1s* and N *1s* regions in XPS study are either 1 or 0.96 depending on the temperature. The stoichiometric formulas of the obtained foams were best approximated to BC_2N for 900 °C annealing and BC_4N for 1100 °C annealing, which reflect the observed 1:1 ratio of boron and nitrogen bonding in the BN domains. Other bonding arrangements observed in Figure 4, like C-N pyridine, C-N graphitic, and boron oxide,are likely defects in the B-C-N structures. The incorporation of these defects provides deviation of the BC_2N and BC_4N formulas as indicated with the fractioned stoichiometric coefficients in Table 1. XPS studies were also done on the powder samples made by milling B-C-N foam (post treatment) samples for 15 min in a pestle and mortar. The boron and nitrogen contents were found to be 3–4 at% B and 2–3 at% N, which were much less than those in the foam samples.This result suggests that the chemical modification is largely confined to the surfaces of the foam, and that pulverization exposes interior regions of the foam ligaments that are predominantly carbon. Consequently, a complete descriptor for the entire material would be carbon@B-C-N composite foam.

Above 900 °C the carbon content was found to increase in contrast to the studies by Han et al.[14] and Portehault et al.[27] who observed a decrease in carbon content with increased temperature. At higher temperatures, B and N atoms likely diffuse deeper into the carbon core to substitute for carbon atoms. Therefore, B and N are diluted into the C core, and the C content near the foam surface (probed by XPS to less than 10 nm depth) increases. The presence of B-C bonds for annealing temperatures of 900 °C and 1100 °C is attributed to the microwave-assisted heat treatment, because boron carbide bonds were only observed for samples with the longest duration (30 min) of microwave treatment. The shorter treatment time (5 min) and annealing alone did not produce boron carbide bonds. XPS could not detect any trace of B-C bonds near the surface of samples without microwave treatment even after these were annealed at temperatures as high as 1500 °C and 2000 °C. On the other hand, the B-C bond fraction in the B *1s* spectra (Figure 4) decreased for the sample annealed at 1100 °C after a maximum value at 900 °C for 30 min microwave treatment. This finding could be caused by rearrangement of B-N domains towards a more stable and segregated state between BN and C domains, where the fraction of B-C bonds is reduced because such developed BN domains are predominantly connected to surrounding hexagonal carbon through N-C bonds.

XRD patterns (**Figure 5**a) reveal that the characteristic hexagonal carbon peaks broaden and shift towards lower diffraction angles upon boron and nitrogen incorporation. Figure 5a shows diffraction patterns for B-C-N foams with 30 min microwave treatment whereas Figure 5b shows the diffraction peaks for (002) planes for carbon and B-C-N foams. The (002) diffraction peak of B-C-N indicates several new shoulders at lower angles along with a graphitic peak (interplanar distance = 3.36 Å). The peaks at lower diffraction angles might have arisen from the different species, e.g., B-C, C-N, B-N and B_2O_3, present within the foam lattice due to chemical treatment (interplanar distance d = 3.44 Å).[33] This result corroborates the incorporation of B and N into graphitic planes of carbon foam because B and N atoms are larger and smaller than C atoms respectively, and changes in inter-planar separations for B-C-N foam as observed here would be expected.[34]

Representative Raman spectra of B-C-N foams together with that of carbon foam are shown in **Figure 6**a for 30 min microwave-treated B-C-N foams annealed at different temperatures. The three dominant peaks are D, G and 2D bands located at ~1332, 1582, 2678 cm^{-1} respectively. The D and 2D band represent lattice defects. These two bands originate from phonons near the Brillouin zone boundary due to double resonance processes.[35] The G band is generally observed in single crystal graphite and represents the in-plane vibrations of nearest neighbors in a graphene layer.[36] A clear shoulder (called D′ band) at 1620 cm^{-1} is apparent, particularly for B-C-N foam annealed at 1100 °C that is also associated with the lattice defects. This band is the double resonance of phonons near the Brillouin zone center.[36] The Raman spectra of 5 min microwave-treated B-C-N foams annealed at different temperatures (not shown) are similar to Figure 6a. For both 5 and 30 min treatments, the Raman spectra with the material annealed at lower temperatures (500 °C and 700 °C) show fluorescence effects that vanish for samples annealed at higher

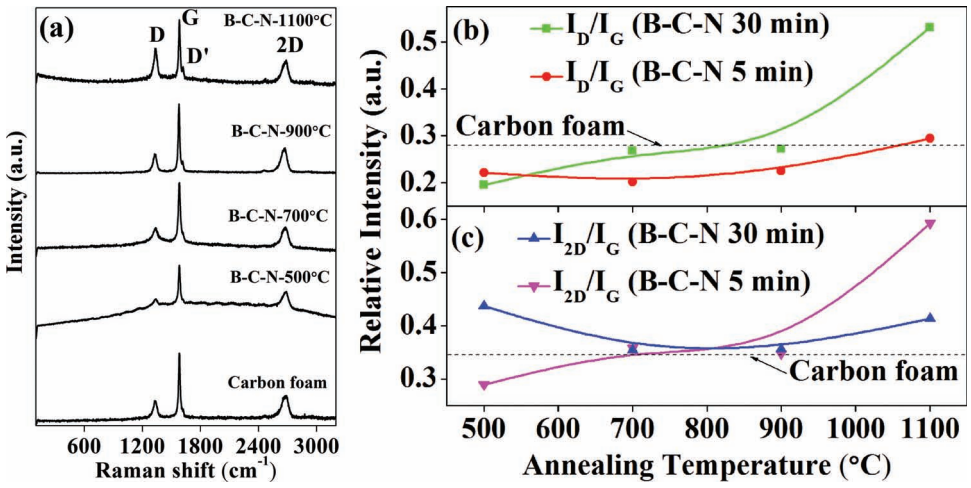

Figure 6. a) Raman spectra of B-C-N foams annealed at different temperatures treated with microwave for 30 min. Variations of I_D/I_G (b) and I_{2D}/I_G (c) with different annealing temperatures of B-C-N foam for 5 min and 30 min microwave treatment.

temperatures (900 °C and 1100 °C). This fluorescence might be due to the presence of unreacted chemicals within the foams annealed at lower temperatures.

The intensity ratio of D and G peaks (I_D/I_G) is a measure of the defect sites in graphitic materials.[37] The variation of I_D/I_G and I_{2D}/I_G ratios of B-C-N foams with annealing temperature for 5 min and 30 min microwave treatment are shown in Figure 6b and **Figure 7**c respectively. The I_D/I_G ratio slightly increases with temperature below 900 °C. For 30 min microwave treatment, the foam also exhibits a significant increasein I_D/I_G at 1100 °C, suggesting that the B-C-N surface layers became more defective with annealing at higher temperatures. This result may be caused by the breaking of unreacted boric acid or boron oxides and the subsequent reaction with the carbon foam surface to form domains of B-N. A similar correlation between I_D/I_G ratio and B-N content in B-C-N nanotubes has been recently reported by Arutyunyan et al.[38] The I_{2D}/I_G value is relatively stable across annealing temperatures for the 30 min microwave treated B-C-N foams. The horizontal lines in Figure 6b,c represent the corresponding values of I_D/I_G and I_{2D}/I_G for carbon foam. Only at 1100 °C the I_D/I_G and I_{2D}/I_G ratios are found to be greater than that of carbon foam. The B-C-N foams annealed at lower temperatures may tend to retain unreacted chemical reagents and boron oxides at surface defect states of the carbon foams substrate. With increased annealing temperatures those chemical reagents and boron oxides are reacted, distorting the carbon domains in order to create BN domains. Consequently, the high temperature annealed B-C-N foams are much more defective than the original carbon foam. This suggestion is supported by the FESEM images (Figure 1d, f) as well as XPS analysis.

The adsorption enthalpies of the carbon and B-C-N foams were evaluated with differential scanning calorimetry.[39] An empty aluminum edge-sealed pan was used as the reference, and another edge-sealed aluminum pan with a top pinhole (diameter = 1 mm) was filled with foam material and methanol. Figure 7a shows the endothermic differential enthalpy of carbon and B-C-N foams with 30 min microwave treatment and annealed at 500 °C and 1100 °C temperatures. There are clear shoulders for desorption of methanol (Figure 7a) molecules for B-C-N foams at higher temperatures, and the overall temperature range of phase change and desorption increases for B-C-N foams.

Desorption enthalpy was calculated by subtracting the enthalpy of only methanol evaporation obtained from separate experiment without any foam material with it. The variations of desorption enthalpies for B-C-N foams annealed at different temperatures with 5 min and 30 min microwave treatments are shown in Figure 7b. The horizontal line in this figure represents the adsorption enthalpy of methanol with as-received pure carbon foam. The desorption enthalpies for B-C-N foams with 5 min microwave treatment are higher than that for carbon foam for all annealing temperatures considered, and the relative increase in enthalpy is relatively insensitive to annealing temperature. The desorption enthalpy of B-C-N foam annealed at 500 °C with 30 min microwave treatment is slightly less than that of the carbon foam. This may be due to the presence of unreacted chemical reagents and boron oxides within that B-C-N foam as indicated by the XPS study. The desorption enthalpy can be influenced by the surface oxidation state.[27,40,41] For annealing temperatures below 900 °C both oxygen content (Figure 2d) and B-O bond presence (Figure 4a) were significant in this regard. However, with higher annealing temperatures the unreacted chemicals were removed and oxides were significantly reduced to form a highly surface defective solid composite of hexagonal BN and carbon domains. B-C-N foam with 30 min microwave treatment and annealed at 1100 °C was found to have the highest desorption enthalpy nearly twice that of methanol on carbon foam. This foam also possesses the highest defective site density on its surface as indicated by FESEM images and Raman studies as well as high B-N content measured by XPS analysis. The interface regions between B-N and graphene (C-C) in B-C-N foams, i.e., B-C and C-N bond regions are the most probable sites for enhanced adsorption due to presence of charged states and charge sharing among B, C and N atoms.

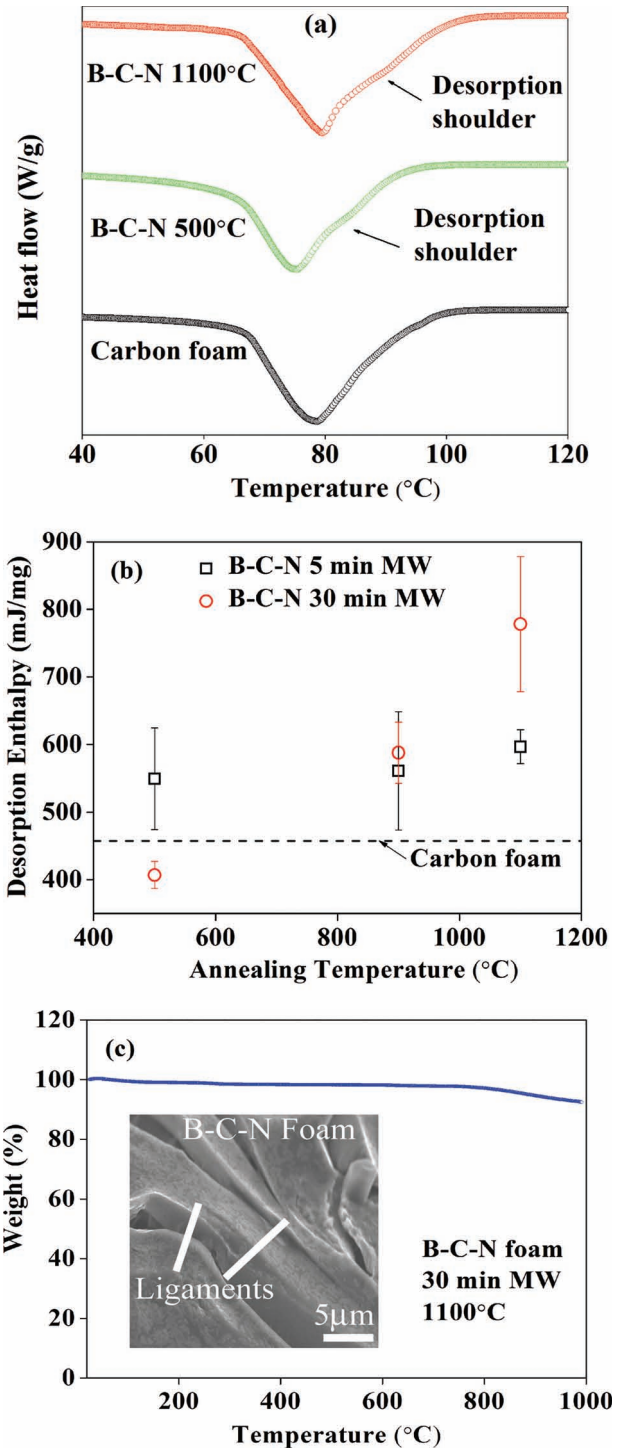

Figure 7. a) Comparison of DSC scans for B-C-N foams annealed at 500 °C and 1100 °C after 30 min microwave treatment with that of carbon foam. b) Variation of methanol adsorption enthalpy of B-C-N foams with annealing temperature. c) Thermogravimetric analysis of B-C-N foam of 30 min microwave treatment and annealed at 1100 °C (Inset: ligaments of same B-C-N foam).

In order to estimate the relative hybrid interatomic bonding (B-C or C-N) between B-N and graphene domains, we have estimated the atomic percentage of B-C and C-N bonds within B-C-N foams from the XPS analysis. These estimations were done by calculating the relative areas under the B-C and C-N peaks in B1s and N1s spectrum respectively, and then the total hybrid bonding percentage was obtained by adding these two (B-C and C-N) contributions. The B-C-N foams treated in microwave for 30 min and annealed at 1100 °C result in BC_4N structures with 8.4 at% hybrid bonding, while this value is 6.1 at% in B-C-N foam obtained through 5 min microwave treatment and annealed at 1100 °C. Hence the observed increment in desorption enthalpy between two similar BC_4N structured B-C-N foams appears to be correlated to this metric. We note that the reported specific surface area for this type of graphitic carbon foam is 20000 m^2 m^{-3} with a density of 0.25-0.6 g cc^{-1} and 75% porosity.[42]

Boron and nitrogen incorporation have considerably increased the active adsorption sites in carbon foam, and an enhancement of desorption enthalpy was observed for B-C-N foam, providing a new adsorbent-adsorbate pair for thermal sorption applications. For thermal storage applications, the thermal stability of the B-C-N foams is an important practical attribute. Results of thermogravimetric analysis (TGA) for B-C-N foam (Figure 7c) treated 30 min in microwave and annealed at 1100 °C reveals no measurable weight loss of the sample in heating up to 1000 °C, thus confirming prior results on powder samples.[43] The intact foam ligaments even after chemical treatment (inset of Figure 7c) with modified surface activation by B and N doping have been achieved. We have also measured the thermal stability of the foams in air atmosphere (not shown here). The pure carbon foam started degrading at 570–580 °C while the B-C-N foam with 30 min microwave treatment and annealed at 1100 °C exhibited thermal stability up to 780 °C. Raidongia et al.[22] reported a degradation of B-C-N layers near 600 °C. This may open other applications for B-C-N foams in addition to the thermal energy storage explored here. Activated carbon with methanol is a well known adsorbate-adsorbent material pair for adsorption cooling applications.[44] In this context the high adsorption enthalpy of the synthesized B-C-N foam compared to pure carbon foam with methanol and its excellent thermal stability suggest that the reported material is a promising candidate for adsorption-assisted thermal cooling,[45] heat regeneration,[46] waste heat recovery,[21,47] and energy storage applications.[28]

3. Conclusion

Boron carbon nitride (B-C-N) foam was has been synthesized by converting the surface of highly porous graphitic carbon foam in a combined microwave-activated chemical-thermal treatment. Microwave treatment had helped to activate surface chemical reactions, and the annealing temperature of 900 °C was found to be sufficient to provide foams with stoichiometries between BC_2N and BC_4N. XPS and XRD results suggest that the treatment produces B-C-N foams that consist predominantly of domains of hexagonal B-N and carbon with some nitrogen substitution in carbon domains. The XPS results also indicate that unreacted chemicals as well as the oxygen content within the B-C-N foam was dependent on the post annealing temperature, with an optimum temperature in the 900–1100 °C range.

B-C-N surface treated foam showed increased adsorption enthalpy with methanol as calculated through DSC experiments. This behavior was correlated to increased surface roughness, hexagonal lattice intercalation and straining, surface defects, and disorder at the boundaries between BN and carbon domains as evidenced by SEM, XRD, Raman, and XPS. The B-C-N foams were demonstrated to have an excellent thermal stability and are suggested as candidate materials for sorption cooling and thermal storage applications using methanol as the adsorbate.

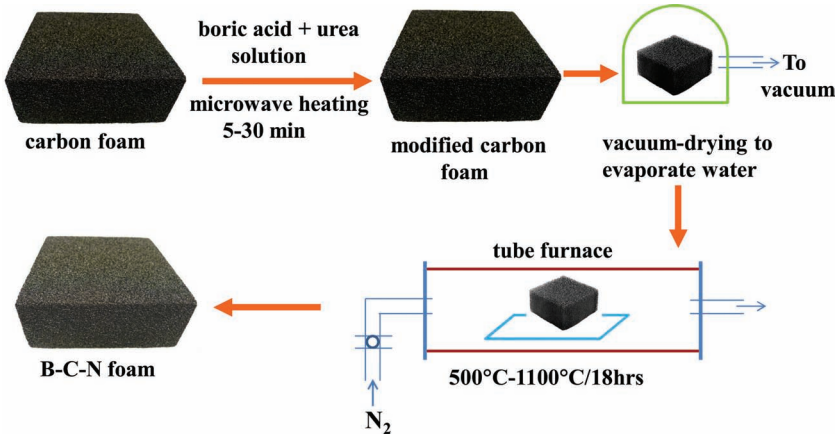

Scheme 1. Schematic synthesis procedure of B-C-N foam from carbon foam.

4. Experimental Section

Graphitic carbon foam, KFOAM (Manufacturer: Koppers Inc., Pittsburgh), of approximately 75 percent open porosity was used as the starting material. The foam ligaments possess high graphitic microstructure of graphitic planes oriented along the axial direction of the foam ligaments was used as the starting material. Foam samples of 8 mm × 8 mm × 10 mm size were chemically treated to synthesize B-C-N foam through steps indicated by schematics shown in **Scheme 1**. Homogeneous solution of boric acid $[B(OH)_3]$ and urea $[CO(NH_2)_2]$ in 1:24 molar proportion (0.5 g and 12 g respectively) in de-ionized (15 mL) water was prepared. The carbon foam in the foregoing solution was placed into a quartz vial (10-20 mL) inside a microwave synthesizer (Biotage Initiator, NC, USA) for treating with microwave irradiation at 20 bar pressure and 120 °C temperature using 400 W power (2.45 GHz) for 5 min and 30 min. The synthesis parameters were controlled automatically by the instrument to maintain the pressure and temperature inside the vial. After chemical treatment, samples were vacuum dried for 12 hours using a vacuum desiccator. The dried samples were heat treated at four different temperatures: 500 °C, 700 °C, 900 °C and 1100 °C for 6 to 18 h in continuous N_2 gas (30 psi) flow to assess the effects of annealing temperature on the B-C-N stoichiometry, residual oxygen content, as well as the removal of unreacted chemicals originating from boric acid and urea.

The surface morphology of B-C-N foam samples was investigated by a field emission scanning electron microscope (FESEM; Hitachi S4800). Chemical composition was investigated by X-ray photoelectron spectroscopy (XPS) using a Kratos Axis Ultra DLD spectrometer with monochromatic Al Kα radiation ($h\nu$ = 1486.58 eV). Survey and high-resolution spectra were collected from a 700 × 400 μm^2 spot size at normal direction with respect to the sample surface. Fixed analyzer pass energies of 160 and 20 eV were used for the survey and high-resolution spectra, respectively. XPS data were analyzed with commercially available CasaXPS software (www.casaxps.com), and individual peaks were fitted to a Gaussian-Lorentzian (GL) function. A charge neutralizer was used for B-C-N foams due to their low electrical conductivity, and the resulting spectra were then corrected on the binding energy scale using the position of the main C 1s component at 284.5 eV as a reference for graphitic carbon [28].

The crystalline nature of the graphitic carbon and B-C-N foams were evaluated using a Bruker D8 Focus X-Ray Diffractometer equipped with Cu K(alpha) x-ray source, 3 circle goniometer and lynseye 1D detector with and without rotation (15 rpm) of the substrate holder.

Raman spectra were collected using a SENTERRA confocal Raman system (Bruker Optics Inc., Billerica, MA) with a 50× air objective at 633 nm laser excitation. The laser power and accumulation time were 20 mW and 10 s.

A differential scanning calorimeter (TA, Q100, V9.8) was used to evaluate the adsorption/desorption enthalpies of the carbon and B-C-N foams for methanol adsorption in a edge-sealed aluminum pan with a top pinhole through a ramped temperature process (–20 °C to 150 °C) at a rate of 20 °C min^{-1}. The pinhole helped to minimize boiling point drift caused by increased pressure inside the pan during the temperature ramp. The nitrogen flow during the experiment was 50 mL min^{-1}. The heat of evaporation of methanol without foam was also recorded under identical settings for comparison by adding only methanol to the pan. The carbon or B-C-N foam was placed in the pan (with pinhole) together with methanol. The stability of the B-C-N foam against thermal degradation was assessed by thermal gravimetric analysis (TA, Q500, V6.7) using an alumina pan by ramping the temperature from 20 °C to 1000 °C at a rate of 20 °C min^{-1} in N_2 atmosphere.

Acknowledgements

The authors are thankful to the U.S. Air Force Research Laboratory (AFRL), and its Office of Scientific Research (AFOSR) under the MURI program on Nanofabrication of Tunable 3D Nanotube Architectures (PM: Dr. Joycelyn Harrison), for financial support in this work. The authors are also grateful to Dr. K. L. Strong, Dr. P. Shamberger and Dr. S. Ganguli, AFRL for their advice. Thanks are due to Prof. R. B. Pipes and C. R. Misiego of Chem. Engg., Purdue University for their excellent help in the DSC and TGA study. The authors are thankful to all the Birck Nanotechnology Center staff for their assistance and cooperation.

Received: February 2, 2012
Revised: March 19, 2012
Published online: May 18, 2012

[1] K. Suenaga, C. Colliex, N. Demoncy, A. Loiseau, H. Pascard, F. Willaime, *Science* **1997**, *278*, 653.
[2] L. Liao, K. Liu, W. Wang, X. Bai, E. Wang, Y. Liu, J. Li, C. Liu, *J. Am. Chem. Soc.* **2007**, *129*, 9562.
[3] C. Zhi, Y. Bando, C. Tang, H. Kuwahara, D. Golberg, *Adv. Mater.* **2009**, *21*, 2889.
[4] D. Golberg, Y. Bando, Y. Huang, T. Terao, M. Mitome, C. C. Tang, C. Y. Zhi, *ACS Nano* **2010**, *4*, 2979.
[5] R. Badzian, *Proc. 3rd Int. Conf. Chem. Vapor Deposition* (Ed: F. A. Claski) American Nuclear Society, Hinsdale, IL **1972**, p. 747–753.
[6] Y. Wada, Y. K. Yap, M. Yoshimura, Y. Mori, T. Sasaki, *Diam. Relat. Mater.* **2000**, *9*, 620.
[7] M. K. Lei, Q. Li, Z. F. Zhou, I. Bello, C. S. Lee, S. T. Lee, *Thin Solid Films* **2001**, *3891*, 194.
[8] D. H. Kim, E. Byon, S. Lee, J. K. Kim, H. Ruh, *Thin Solid Films* **2004**, *447–448*, 192.
[9] R. Gago, I. Jimenez, J. M. Albella, *Thin Solid Films* **2000**, *373*, 277.

[10] P.-C. Tsai, *Surf. Coat. Technol.* **2007**, *201*, 5108.
[11] T. Yuki, S. Umeda, T. Sugino, *Diam. Relat. Mater.* **2004**, *13*, 1130.
[12] J. Yu, E. G. Wang, J. Ahn, S. F. Yoon, Q. Zhang, J. Cui, M. B. Yu, *J. Appl. Phys.* **2000**, *87*, 4022.
[13] Y. K. Yap, in *Encyclopedia of Nanoscience and Nanotechnology*, Vol *1*, (Ed: H. S. Nalwa) American Scientific Publishers, Stevenson Ranch, CA **2004**, p. 383–394.
[14] W. Han, Y. Bando, K. Kurashima, T. Sato, *Jpn. J. Appl. Phys.* **1999**, *38*, L755.
[15] X. Blase, J.-C. Charlier, A. D. Vita, R. Car, X. Blase, J.-C. Charlier, A. D. Vita, R. Car, *Appl. Phys. Lett.* **1997**, *70*, 197.
[16] W. Q. Han, H. G. Yu, Z. Liu, *Appl. Phys. Lett.* **2011**, *98*, 203112.
[17] K. Anupam, A. Chatterjee, G. N. Halder, S. C. Sarkar, *Chem. Eng. J.* **2011**, *1771*, 541.
[18] R. Wang, R. G. Oliveira, *Int. Sorption Heat Pump Conf.* June 22–24, **2005** Denver, CO, USA.
[19] B. Li, Z. Lei, X. Zhang, Z. Huang, *Catal. Today* **2010**, *158*, 515.
[20] K. Sumathy, K. H. Yeung, L. Yong, *Prog. Energy Comb. Sci.* **2003**, *29*, 301.
[21] Q. Xiaoni, L. Zhenyan, *Adv. Mater. Res.* **2011**, *233–235*, 2486.
[22] K. Raidongia, A. Nag, K. P. S. S. Hembram, U. V. Waghmare, R. Datta, C. N. R. Rao, *Chem. Eur. J.* **2010**, *16*, 149.
[23] A. L. Myers, P. A. Monson, *Langmuir* **2002**, *18*, 10261.
[24] N. C. Gallego, J. W. Klett, *Carbon* **2003**, *41*, 1461.
[25] J. Kletta, R. Hardyb, E. Rominec, C. Wallsa, T. Burchella, Carbon **2000**, *38*, 953.
[26] L. M. Kustov, I. M. Sinev, *Russ. J. Phys. Chem. A* **2010**, *84*, 1676.
[27] D. Portehault, C. Giordano, C. Gervais, I. Senkovska, S. Kaskel, C. Sanchez, M. Antonietti, *Adv. Funct. Mater.* **2010**, *20*, 1827.
[28] D. Briggs, J. T. Grant, *Surface analysis by Auger and X-ray photoelectron spectroscopy*, IM Publications, Chichester UK **2003**.
[29] A. R. Burke, C. R. Brown, W. C. Bowling, J. E. Glaub, D. Kapsch, C. M. Love, R. B. Whitaker, W. E. Moddeman, *Surf. Interface Anal.* **1988**, *11*, 353.
[30] R. Trehan, Y. Lifshitz, J. W. Rabalais, *J. Vac. Sci. Technol. A* **1990**, *8*, 4026.
[31] S. Y. Kim, J. Park, H. C. Choi, J. P. Ahn, J. Q. Hou, H. S. Kang, *J. Am. Chem. Soc.* **2007**, *129*, 1705.
[32] A. A. Voevodin, J. G. Jones, J. S. Zabinski, Zs. Czigány, L. Hultman, *J. Appl. Phys.* **2002**, *92*, 4980.
[33] F. Zhuge, Z. G. Ji, H. P. He, Z. Z. Ye, L. P. Zhu, *J. Cryst. Growth* **2008**, *310*, 3869.
[34] M. Hubacek, T. Sato, *J. Solid State Chem.* **1995**, *114*, 258.
[35] E. B. Barros, N. S. Demir, A. G. Souza Filho, A. Jorio, G. Dresseihaus, M. S. Dresselhaus, *Phys. Rev. B* **2005**, *71*, 165422.
[36] C. Thomsen, S. Reich, *Phys. Rev. Lett.* **2000**, *85*, 5214.
[37] R. Paul, S. N. Das, S. Dalui, R. N. Gayen, R. K. Roy, R. Bhar, A. K. Pal, *J. Phys. D: Appl. Phys.* **2008**, *41*, 055309.
[38] N. R. Arutyunyan, R. Arenal, E. D. Obraztsova, O. Stephan, A. Loiseau, A. S. Pozharov, V. V. Grebenyukov, *Carbon* **2012**, *50*, 791.
[39] G. I. Makhatadze, *Curr. Protoc. Protein Sci.* **2001**, 7.9.1.
[40] S. H. Jhi, Y. K. Kwon, *Phys. Rev. B* **2004**, *69*, 245407.
[41] J. Pattanayak, T. Kar, S. Scheiner, *J. Phys. Chem. A* **2002**, *106*, 2970.
[42] K. C. Leong, H. Y. Li, L. W. Jin, J. C. Chai, *J. Heat Transf.* **2011**, *133*, 060902.
[43] K. Raidongia, K. P. S. S. Hembram, U. V. Waghmare, M. Eswaramoorthy, C. N. R. Rao, *Z. Anorg. Allg. Chem.* **2010**, *636*, 30.
[44] R. Z. Wang, J. P. Jia, Y. H. Zhu, Y. Teng, J. Y. Wu, J. Cheng, Q. B. Wang, *J. Solar Energy Eng.* **1997**, *119*, 214.
[45] G. Cacciola, G. Restuccia, L. Mercadante, *Carbon* **1995**, *33*, 1205.
[46] Y. Teng, R. Z. Wang, *Chin. Cryogenics.* **1995**, *85*, 48.
[47] J. Deng, R. Z. Wang, G. Y. Han, *Process Energy Combustion Sci.* **2011**, *37*, 172.